Pergamon

Int. J. Heat Mass Transfer. Vol. 39, No. 15, pp. 3249–3260, 1996

0017–9310/96 $15.00+0.00

PII: S0017–9310(96)00012–9

Turbulent vapor condensation with noncondensable gases in vertical tubes

J. L. MUÑOZ-COBO, L. HERRANZ*, J. SANCHO, I. TKACHENKO and G. VERDÚ

Department of Chemical and Nuclear Engineering, Polytechnic University of Valencia, P.O. Box 22012, E-46071 Valencia, Spain

(*Received* 23 *June* 1994 *and in final form* 28 *July* 1995)

Abstract—This paper develops a theory for turbulent vapor condensation in vertical tubes when noncondensable gases are present. The local heat transfer coefficient is calculated and the results are compared with experimental data. Approximate methods to calculate the condensate film thickness with good precision are developed without need to iterate to solve the transcendental equation which obeys the film thickness. A comparison of the theory predictions with some experimental data resulted in a good agreement. Copyright © 1996 Elsevier Science Ltd.

1. INTRODUCTION

It is well known that annular filmwise condensation inside vertical tubes in the presence of noncondensable gases (NC) is an important process in chemical and power industries. A growing interest in this process has arisen due to the design of new types of passive cooling containment condensers for the next generation of nuclear power reactors [1–14].

Pioneering work in this field has been developed by Minkowycz and Sparrow [6, 7], which dealt mainly with condensation in unconfined spaces, such as on flat plates or outside horizontal tubes. The influence of the interfacial shear stress on the condensation has been studied by Rohsenow, Webber and Ling, and by Carpenter and Colburn. These authors, cited in ref. [3], considered also the influence of vapor velocity on film condensation inside tubes.

Minkowycz and Sparrow and Sparrow *et al.* [7] show the influence of noncondensable air on the heat transfer rate in the case when the steam–air mixture was either stagnant or flowing. They obtained reductions in the heat transfer rates due to the presence of small mass fractions of noncondensables, and they observed these reductions becoming more pronounced as the total pressure was reduced. More recently, Wang and Tu [1] have developed a theory to include the effect of small amounts of noncondensable gas on laminar filmwise condensation of a vapor–gas mixture flowing turbulently in a vertical tube. They found that the reductions in heat transfer due to the noncondensable gas were more significant at low pressures, in agreement with Sparrow's results, and at low Reynolds numbers of the mixture.

Experimental studies of condensation inside tubes and channels have been carried out by Borishansky *et al.* [15–17], with and without noncondensable gases included. Also, Kreiden *et al.* [18] measured the pressure drop for the condensing flow of a steam inside a tube. Dehbi [19] performed an experiment on condensation under natural circulation with noncondensable gas. All these results were reported as length averaged heat transfer coefficients.

Recently, new experiments have been designed to yield local values of the heat transfer coefficients, and to permit more detailed design analysis of condensers, such as the passive containment cooling condenser (PCCC), needed for the decay heat removal in passive safety reactors like simplified boiling water reactors (SBWR). Experiments of this type with and without noncondensable gases have been carried out by Vierow and Schrock [9], Kageyama *et al.* [8], Ogg *et al.* [21], Siddique *et al.* [20], and Nagasaka. Also Kageyama, Peterson and Schrock [8] have developed a diffusion layer modeling for condensation in vertical tubes with noncondensable gases.

In a condenser of this type, the axial variation in the bulk noncondensable concentration plays a major role in determining the local heat transfer coefficient. This behavior has been observed by Vierow and Schrock [9], who correlated the 'degradation factor', defined as the ratio of the experimental heat transfer coefficient to the theoretical one given by pure Nusselt theory, with the bulk local NC concentration and the mixture Reynolds number. They found that these local degradation factors decreased with the bulk noncondensable concentration, whereas they increased with the Reynolds number of the vapor–NC mixture. Such behavior was expected for two principal reasons. First, the interfacial shear should tend to reduce the film thickness in downflow, and this fact tends to reduce the thermal resistance of the film. Second, the accumulation of air at the interface reduces the steam partial pressure, depresses the interface temperature

* Institute of Nuclear Technology, CIEMAT, Avda, Complutense 22, E-28040 Madrid, Spain.

NOMENCLATURE

c_m	molar concentration of the mixture of steam and noncondensable gases
C_p	specific heat at constant pressure
d	inner diameter of the tube
d_H	hydraulic diameter of the vapor-noncondensable gases mixture
D	diffusion coefficient
f	friction factor
g	gravity acceleration
G_m	mass flux of vapor and noncondensables mixture
h_c	condensation heat transfer coefficient
h_t	total heat transfer coefficient
h_s	sensible heat transfer coefficient through the diffusion layer
h_{fg}	latent heat of vaporization
j_v	mass flux of vapor toward the interface
K_v	vapor mass transfer coefficient
k	thermal conductivity
k_c	effective condensation thermal conductivity
$m_s(j)$	steam mass flow rate entering into element j
M	molecular weight
p	local pressure
q''	heat flux
R	radius
Re	Reynolds number
Sc	Schmidt number
Sh	Sherwood number
T	temperature
u_z	liquid film velocity in the axial direction
u_m	mixture velocity in the axial direction
v	radial component of velocity
v_{fg}	difference in specific volume between saturated liquid and vapor
w_a	noncondensables mass fraction in the bulk
x	molar fraction
y	coordinate, see Fig. 1
z	axial distance.

Greek symbols

Γ	condensate mass flow rate per unit of circular length
δ	condensate film thickness
μ	dynamic viscosity
ν	kinematic viscosity
ρ	density
τ	shear stress.

Subscripts

a	noncondensable
b	bulk region
f	liquid
i	liquid-gas interface
m	vapor-noncondensable gas mixture
s	sensible
v	vapor phase
w	wall.

and thereby reduces the condensing heat transfer coefficient.

The main factors that should be taken into account in any condensation heat transfer model inside tubes with noncondensable gases are:

(i) Interfacial shear stress. This effect is very important at high Reynolds number of the vapor–NC mixture, and increases with the square of the relative velocity between the mixture and the interface of the condensing film.

(ii) The noncondensable gases concentration significantly modifies the mechanism of condensation for concurrent downflow in vertical tubes. The noncondensable gas is carried with the vapor towards the interface, where it accumulates. This concentration gradient produces a driving force that yields gas diffusion away from the interface.

(iii) The waviness of the liquid film can also influence the condensation heat transfer coefficient, even at relatively low film Reynolds numbers.

(iv) Mist formation increases the sensible heat transfer coefficient through the diffusion boundary layer.

(v) The interfacial shear stresses acting on the liquid and the vapor, respectively, are affected in a different way by the condensation process.

There are other minor effects which will be discussed throughout the paper.

The goal of the paper is to elaborate a model, which will predict adequately the local condensation heat transfer coefficients inside vertical tubes when different mass fractions of noncondensable gases are present.

The paper is organized as follows: Section 2 is devoted to the development of the heat transfer model without noncondensables, and the various approximations that can be made to simplify the calculations. Also, this section deals with the model of noncondensable gases in the turbulent and laminar regions, as well as the combination of this model with the model previously developed. Section 3 deals with the practical implementation of the method of calculation, and the comparison with the experimental data. Finally, in Section 4 the main conclusions of this work are outlined, as well as some addresses where it

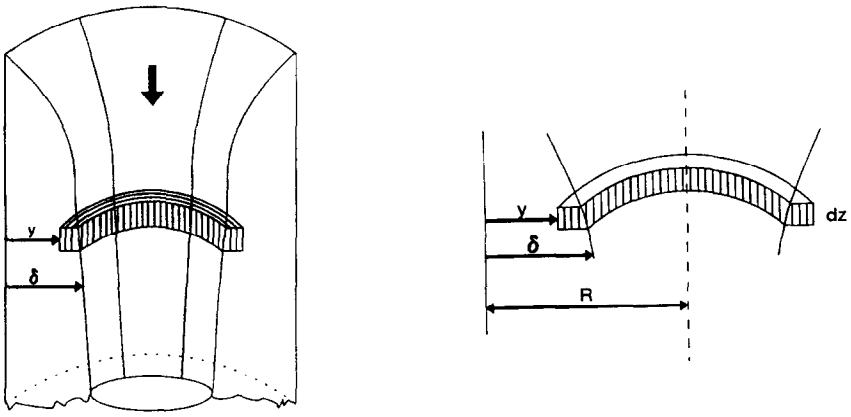

Fig. 1. Condensate film element, to perform the force balance.

would be necessary to carry out further experimental research in order to improve the model predictions.

2. THE PHYSICAL MODEL

Development of the model

Consider steady, filmwise condensation of a downflow vapor–NC gas mixture in a vertical tube. The mixture regime can be either laminar or turbulent, depending on the position considered. Near the tube entrance, and in the upper region of the tube the regime will be turbulent, whereas in the lower region when most of the vapor has condensed the regime will be laminar. The effect of noncondensable gases on the interfacial temperature will be considered by means of a diffusion layer modeling that will be displayed later in this section. We assume also that the flow of condensate in the film is laminar, and that the vapor entering the tube is saturated and flows with a fully developed profile.

Let us choose a height z, measured from the entrance of the tube, to calculate the local condensation heat transfer coefficient. Then consider a force balance on the element of condensate film displayed at Fig. 1, lying radially between y and δ, and axially between z and $z+\mathrm{d}z$; we have

$$\pi\{(R-y)^2-(R-\delta)^2\}\rho_f g\,\mathrm{d}z - \pi\{(R-y)^2-(R-\delta)^2\}\frac{\mathrm{d}p}{\mathrm{d}z}\mathrm{d}z + \tau_{if}2\pi(R-\delta)\,\mathrm{d}z = \mu_f\frac{\mathrm{d}u_Z}{\mathrm{d}y}2\pi(R-y)\,\mathrm{d}z, \tag{1}$$

where p is the local pressure, $u_Z(y)$ is the axial component of the velocity at radial position y, μ_f is the dynamic viscosity of the fluid, and τ_{if} is the shear stress acting on the liquid at the interface. The local pressure gradient is expressed in the form [3]

$$\frac{\mathrm{d}p}{\mathrm{d}z} = \rho_m^* g, \tag{2}$$

where ρ_m^* is a fictitious mixture density, that will be computed later by performing a force balance on an element of vapor. Now, rearranging and integrating equation (1), with the nonslip condition at the wall interface, one gets the velocity distribution $u_Z(y)$

$$u_Z(y) = \frac{g}{2\mu_f}\left[Ry-\frac{y^2}{2} + (R-\delta)^2\ln\left(1-\frac{y}{R}\right)\right](\rho_f-\rho_m^*) - \frac{\tau_{if}}{\mu_f}(R-\delta)\ln\left(1-\frac{y}{R}\right). \tag{3}$$

The mass flow rate per unit of circular length $\Gamma(z)$ is computed (Fig. 2)

$$\Gamma(z) = \frac{\int_0^{\delta(z)} 2\pi(R-y)\rho_f u_Z(y)\,\mathrm{d}y}{\pi d}. \tag{4}$$

The next step is to apply the conservation of momentum to the mixture volume element displayed at Fig. 3. This calculation yields the following result:

$$\pi(R-\delta)^2\rho_m g\,\mathrm{d}z - \tau_{im}2\pi(R-\delta)\,\mathrm{d}z - \frac{\mathrm{d}p}{\mathrm{d}z}\pi(R-\delta)^2\,\mathrm{d}z - \frac{\mathrm{d}}{\mathrm{d}z}(\rho_m u_m^2)\pi(R-\delta)^2\,\mathrm{d}z = 0 \tag{5}$$

where u_m is the mixture velocity and τ_{im} the interfacial shear acting on the mixture. From equation (5) and on account of expression (2), the fictitious mixture density is obtained

$$\rho_m^* = \rho_m\left\{1+\frac{1}{\rho_m g d_H}\left(4\frac{\mathrm{d}}{\mathrm{d}_H}u_m\frac{\mathrm{d}\Gamma}{\mathrm{d}z} - 4\tau_{im} - d_H G_m\frac{\mathrm{d}u_m}{\mathrm{d}z}\right)\right\}. \tag{6}$$

Here d_H is the hydraulic diameter of the vapor–NC mixture flow given by

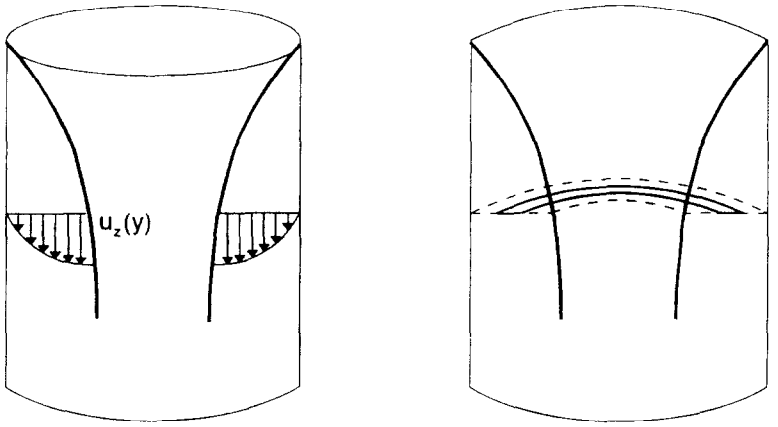

(a) (b)

Fig. 2. (a) Velocity distribution $u_Z(y)$; (b) element of area used in the determination of the mass flow rate per unit of circumference.

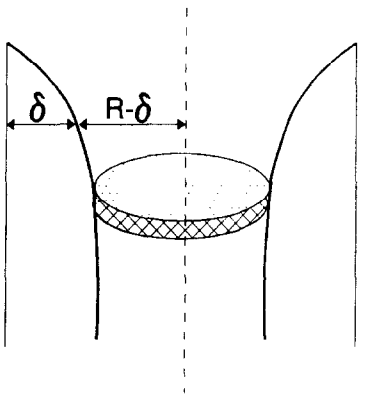

Fig. 3. Typical mixture (steam and noncondensables) volume element, used to apply the momentum conservation.

$$d_H = d - 2\delta. \tag{7}$$

The interfacial shear stresses τ_{im} and τ_{if} acting on the mixture and liquid, respectively, are different due to the influence of condensation. This influence has been studied by Silver [22], Wallis [23], and Spalding [24]. The interfacial shear stresses are calculated using the following expressions:

$$\tau_{im} = \tau_{io}\frac{a'}{e^{a'}-1} \tag{8}$$

$$\tau_{if} = \tau_{io}\frac{a'e^{a'}}{e^{a'}-1}, \tag{9}$$

where τ_{io} is the interfacial shear stress in the absence of phase change, given by

$$\tau_{io} = f_i \tfrac{1}{2}\rho_m(u_m - u_i)^2, \tag{10}$$

where u_i is the velocity of the liquid at the interface, and f_i is the friction factor at the interface. Finally, a' is the ratio of the mass flow rate condensing per unit area in the tube $d\Gamma/dz$, to the mass flux hitting the interface and rebounding after giving up its momentum to the surface. This quotient can be approximated by

$$a' = \frac{\dfrac{d\Gamma}{dz}}{\rho_m f_i(u_m - u_i)/2}. \tag{11}$$

Observe that from equations (8) and (9) one arrives expanding $e^{a'}$ up to the second order in a', to the Silver and Wallis formulas based on Reynolds analogy [22, 23].

The interfacial friction factor f_i, is crucial in the determination of the interfacial shear stress, which strongly influences the condensate film thickness at high Reynolds numbers. The factor f_i was calculated using the Wallis' expression [23], which depends on film thickness, and is given by

$$f_i = f_m\left(1 + 360\frac{\delta}{d}\right), \tag{12}$$

where f_m is the friction factor of the vapor–NC mixture for smooth tube wall

$$f_m = 0.079 Re_m^{-0.25} \quad Re_m > 2300 \tag{13}$$

$$f_m = \frac{16}{Re_m} \quad Re_m < 2300 \tag{14}$$

where Re_m is the Reynolds Number of the mixture. It was checked that the expression (12) works well at low pressures, but at high pressures some authors [25] suggest using another expression or performing further research.

To obtain the local mass rate of condensation per unit area which appears in equations (6) and (11), we equate the conduction heat flux rate through the condensate film to the energy flux rate due to the

vapor condensation and subcooling to the average condensate film temperature, plus the sensible heat flux rate transferred through the interface

$$k_f \frac{\Delta T}{\delta} = \frac{d\Gamma}{dz} h'_{fg} + k_{m,i}\left(\frac{\partial T}{\partial y}\right)_i \tag{15}$$

with

$$\Delta T = T_i - T_w \tag{16}$$

and

$$h'_{fg} = h_{fg} + 0.68 C_{pf} \Delta T, \tag{17}$$

where T_i and T_w are the interface and wall temperatures, respectively, h_{fg} is the latent heat of vaporization, C_{pf} is the specific heat of liquid phase, and $k_{m,i}$ is the mixture thermal conductivity at the interface. h'_{fg} includes two terms; the first one is the latent heat of vaporization, and the second one is the subcooling average energy of the condensate. This expression was deduced by Rohsenow [34], on account of the nonlinear temperature distribution through the condensate film.

To obtain the unknown interface temperature, we use a diffusion boundary layer model [4, 8], see Fig. 4. The noncondensable gas is carried with vapor toward the interface where it accumulates, in this way the partial pressure of the NC gas at the interface increases above that in the bulk of the mixture. Assuming [3] that the temperatures at the interface and the diffusion boundary layer correspond to the saturation temperature equivalent to the partial pressure of the vapor p_v, i.e. $T_{sat}(p_v)$, one observes in Fig. 4 the variation in temperature through the diffusion boundary layer.

The sensible heat flux at a distance y from the interface, and inside the diffusion boundary layer, is made up of two components: a conductive heat transfer term and a convective heat transport term

$$q''_s = k_m \frac{\partial T}{\partial y} + c_m M_m v C_{pm}(T - T_i), \tag{18}$$

where c_m is the total molar concentration in the mixture, M_m the molecular weight of the mixture, v the radial velocity component (normal to surface) of the mixture and C_{pm} the specific heat at constant pressure of the mixture.

Multiplying equation (18) by the integration factor $\exp[b(y)]$, with $b(y)$ given by

$$b(y) = \int_{y_i}^{y} \frac{c_m M_m v C_{pm}}{k_m} dy, \tag{19}$$

one gets

$$\frac{d}{dy}\left(e^{b(y)}(T - T_i)\right) = \frac{q''_s}{k_m} e^{b(y)}. \tag{20}$$

The integration of equation (20), between the interface ($y = y_i$), and the edge of the diffusion layer ($y = y_i + \delta_D$) gives,

$$q''_s = \frac{k_m}{\delta_D} \frac{a}{1 - \exp(-a)}(T_b - T_i) = h_S(T_b - T_i) \tag{21}$$

with

$$a = \int_{y_i}^{y_i + \delta_D} \frac{c_m M_m v C_{pm}}{k_m} dy = \left(\overline{\frac{c_m M_m v C_{pm}}{k_m}}\right)\delta_D, \tag{22}$$

where the overbar denotes the average operation. The right hand side of expression (22) can be approximated as follows:

$$a \approx \frac{c_m M_m \bar{v} C_{pm}}{k_m} \delta_D. \tag{23}$$

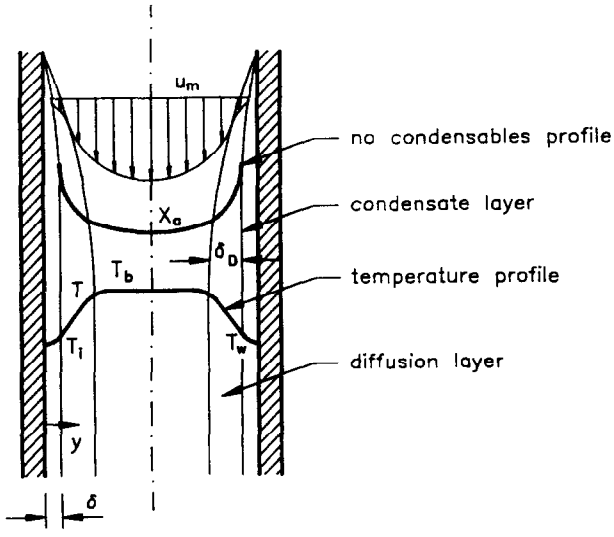

Fig. 4. Schematic diagram of vapor–NC condensation process in vertical tubes with concurrent downflow.

Here c_m, C_{pm}, k_m, are average properties over the diffusion layer, and $\bar{v}$ is the average velocity of the vapor–NC mixture toward the interface.

To calculate $\bar{v}$, one takes into account the fact that at a stationary state the molar concentrations of vapor and NC remain unchanged at a given position y. This means that the convective flux of NC carried with the vapor toward the interface must be compensated by the diffusive NC flux away from the interface,

$$c_m x_a v = -D c_m \frac{\partial x_a}{\partial y}. \tag{24}$$

where x_a is the NC molar fraction, and D is the diffusion coefficient.

From equations (24), the following expression for the absolute average velocity toward the interface is obtained after integration between the diffusion layer limits:

$$\bar{v} = \frac{D}{\delta_D}\frac{x_{a,i}-x_{a,b}}{x_{a,av}} = \frac{D}{\delta_D}\frac{p_{a,i}-p_{a,b}}{p x_{a,av}}. \tag{25}$$

Here $x_{a,av}$ is the log mean of the NC molar fraction, and $p_{a,i}$ and $p_{a,b}$ are the NC partial pressures at the interface and in the bulk, respectively, with $x_{a,av}$ given by

$$x_{a,av} = \frac{x_{a,i}-x_{a,b}}{\ln(x_{a,i}/x_{a,b})}. \tag{26}$$

Next the following obvious substitution is made in equation (25):

$$p_{a,i}-p_{a,b} = p_{v,b}-p_{v,i}, \tag{27}$$

with $p_{v,b}$ and $p_{v,i}$ being the vapor partial pressures at the bulk and in the boundary layer, respectively. Next a modified Clausius–Clapeyron equation [4, 8] is used to provide a relationship between the partial pressure and the saturation temperature at the interface and in the bulk. Proceeding in this way, expression (25) can be recast as follows:

$$\bar{v} = \frac{D h_{fg}}{\delta_D p x_{a,av}}\frac{(T_b-T_i)}{T_{av} v_{fg}}. \tag{28}$$

Here T_{av} is the average temperature in the diffusion layer, and v_{fg} is the difference of specific volumes between saturated liquid and vapor.

The definition of the mass transfer coefficient K_v on account of equation (28) can be rewritten in the form,

$$K_v = \frac{D}{\delta_D} = \frac{\bar{v} p x_{a,av} T_{av} v_{fg}}{(T_b-T_i)h_{fg}}. \tag{29}$$

The Sherwood number [24], suitable for mass transfer processes, is defined as

$$Sh_d = \frac{K_v d}{D} = \frac{\bar{v} p x_{a,av} T_{av} v_{fg} d}{D(T_b-T_i)h_{fg}}. \tag{30}$$

It can be recasted in terms of the condensation heat transfer coefficient h_c, and an effective condensation conductivity k_c,

$$Sh_d = \frac{h_c d}{k_c} = \left[\frac{c_m M_v x_{v,av}\bar{v} h_{fg}}{T_b-T_i}\right] d\left[\frac{p T_{av} v_{fg} x_{a,av}}{D h_{fg}^2 c_m M_v x_{v,av}}\right]. \tag{31}$$

Notice that the first term between brackets is the standard condensation heat transfer coefficient, and the last one is the inverse of an effective condensation thermal conductivity

$$k_c = \frac{D h_{fg}^2 c_m M_v}{p T_{av} v_{fg}}\frac{x_{v,av}}{x_{a,av}}. \tag{32}$$

The total heat flux q''_{t1} through the diffusion boundary layer is made up of the sensible component q''_s, given by equation (21), and the condensation component q''_c, that can be obtained from equation (31). On account of equations (21) and (31) one gets,

$$q''_{t1} = q''_s + q''_c = h_s(T_b-T_i)+h_c(T_b-T_i). \tag{33}$$

This total heat flux through the diffusion boundary layer must be equal to the heat flux through the condensate film,

$$q''_{t2} = \frac{k_f}{\delta}(T_i-T_w). \tag{34}$$

It is well known [1, 4] that one needs to iterate to get the interfacial temperature T_i for which, at the stationary state, the total heat fluxes through the diffusion and the condensate film layer are equal.

To calculate the condensate film thickness δ, which appears in equation (34), one usually neglects the sensible heat transfer term which appears in equation (15). Since the local $\delta(z)$ depends on the axial position, one gets from equation (15), after some trivial calculus followed by an integration from 0 to z, the following transcendental equation in $\delta(z)$:

$$z = \frac{h'_{fg}}{k_f \Delta T}\int_0^{\delta(z)}\frac{d\Gamma}{d\delta'}\delta'\,d\delta', \tag{35}$$

where ΔT is given by expression (16).

For a given z, one has to solve equation (35) to compute $\delta(z)$. Here it was solved by means of the secant algorithm [28], while the integrations have been performed by means of the Tchebichev method of integration based on Tchebichev polynomials [28]. However, an approximate method of solution to be displayed in the next section was developed. It provides results very close to the exact ones, and does not employ iterations to compute $\delta(z)$.

Finally, the heat transfer coefficients h_s and h_c, which appear in equation (33), can be calculated on account of the appropriate correlations which depend on the mixture regime and other properties of the mixture, such as mist formation and so on.

Now, the heat and mass transfer analogy is to be applied, and the Nusselt and Sherwood numbers are correlated in the form

$$Nu_0 = C_1 \quad \text{for laminar flow}, \quad Re < 2300 \tag{36}$$

$$Nu_0 = C_2 Re^{n_1} Pr^{n_2} \quad \text{for turbulent flow,} \quad Re > 2300 \tag{37}$$

$$Sh_0 = C_1 \quad \text{for laminar flow,} \quad Re < 2300 \tag{38}$$

$$Sh_0 = C_2 Re^{n_1} Sc^{n_2} \quad \text{for turbulent flow,} \quad Re > 2300. \tag{39}$$

Here Re, Pr and Sc are the Reynolds, Prandtl and Schmidt numbers, respectively Sh_0 is the single phase mass convection coefficient without mass suction, and Nu_0 is the Nusselt number for single phase sensible heat transfer coefficient without mass suction and mist formation. The coefficients are commonly given the values $C_1 = 4.364$, $C_2 = 0.023$, and $n_1 = 0.8$, $n_2 = 0.35$.

If one includes the suction of mass due to condensation and mist effects, the following result is obtained from equation (21):

$$Nu = \frac{h_s d}{k_m} = C_{mist} \frac{a}{1-\exp(-a)} Nu_0 \tag{40}$$

$$a = \frac{c_m M_m \bar{v} C_{pm}}{h_{s0}} = \frac{j_m C_{pm}}{h_{s0}}. \tag{41}$$

Here $h_{s0} = k_m/\delta_D$, and C_{mist} is a factor to account for the augmentation in sensible heat transfer due to mist formation, as noted by Mori and Hijakata [27], and Peterson *et al.* [4]. Mist formation significantly increases the effective specific heat of the gas–vapor mixture, increasing the effective Prandtl number.

Like the friction factor and the sensible heat transfer coefficient, the Sherwood number related to the mass transfer coefficient is also influenced by condensation occurring at the liquid–gas interface, and therefore an equation similar to equation (40) was suggested by Ackermann [34], and Wang and Tu [1] to account for this effect of condensation mass flux,

$$Sh = C_w \frac{\phi_a}{1-\exp(-\phi_a)} Sh_0. \tag{42}$$

Here the quantity ϕ_a is given by

$$\phi_a = \frac{Re_w Sc}{Sh_0} \tag{43}$$

with $Re_w = v_w d/\nu_m$, where ν_m is the kinematic viscosity. The factor C_w that appears in equation (42) have been attributed by Kageyama *et al.* [8] to the effects of surface roughness due to film waviness.

Taking into account expressions (33), (38) and (42), a total Nusselt number can be determined in terms of experimentally measurable quantities,

$$Nu_t = \frac{q_t'' d/(T_b - T_i)}{k_{ef,t}} = C_2 Re^{n_1} Sc^{n_2}, \quad \text{for } Re_m > 2300, \tag{44}$$

where $k_{ef,t}$ is an effective conductivity for the turbulent regime,

$$k_{ef,t} = k_c C_w \frac{\phi_a}{1-\exp(-\phi_a)} + k_m C_{mist} \frac{a}{1-\exp(-a)} \left(\frac{Pr}{Sc}\right)^{n_2}; \tag{45}$$

$$Nu_t = \frac{q_t'' d/(T_b - T_i)}{k_{ef,l}} = C_1, \quad \text{for } Re_m < 2300, \tag{46}$$

and $k_{ef,l}$ is an effective conductivity for the laminar regime,

$$k_{ef,l} = k_c C_w \frac{\phi_a}{1-\exp(-\phi_a)} + k_m C_{mist} \frac{a}{1-\exp(-a)} \tag{47}$$

with ϕ_a given by expression (43).

Approximate method to compute the condensate film thickness

In order to simplify the calculations within the model developed in the previous section a number of simplifications have been performed. In particular, one first computes $d\Gamma/d\delta$ taking into account equations (3) and (4); this calculation yields

$$\begin{aligned}
\frac{d\Gamma}{d\delta} &= \frac{1}{2R\mu_f} \rho_f (\rho_f - \rho_m^*) g (R-\delta) \\
&\times \left[\delta \left(R - \frac{\delta}{2} \right) + (R-\delta)^2 \ln\left(1 - \frac{\delta}{R}\right) \right] \\
&- \frac{\tau_{if} \rho_f}{R\mu_f} (R-\delta)^2 \ln\left(1 - \frac{\delta}{R}\right) - \frac{\rho_f}{R\mu_f} \\
&\times (\rho_f - \rho_v^*) g (R-\delta) \int_0^\delta (R-y) \ln\left(1 - \frac{y}{R}\right) dy \\
&+ \frac{\tau_{if} \rho_f}{R\mu_f} \int_0^\delta (R-y) \ln\left(1 - \frac{y}{R}\right) dy \\
&- \frac{d\tau_{if}}{d\delta} \frac{\rho_f}{R\mu_f} (R-\delta) \int_0^\delta (R-y) \ln\left(1 - \frac{y}{R}\right) dy \\
&- \frac{1}{2R\mu_f} \rho_f \frac{d\rho_m^*}{d\delta} g \int_0^\delta (R-y) \left[Ry - \frac{y^2}{2} \right. \\
&\left. + (R-\delta)^2 \ln\left(1 - \frac{y}{R}\right) \right] dy.
\end{aligned} \tag{48}$$

Further, expanding $\ln(1-y/R)$ into the Taylor series, and calculating the derivatives $d\tau_i/d\delta$ and $d\rho_m^*/d\delta$ with the help of expressions (8), (10), (12) and (6), an expression for $d\Gamma/d\delta$ has been found. Then this expression was substituted into equation (35), and after an integration the following approximate result

was arrived at, by substituting in the square brackets δ by δ_p:

$$\delta = \frac{1.259(\delta_N^*)^{4/3}}{[\delta_p(a_1 + a_2 x + a_3 x^2) + l_i(b_1 + b_2 x + b_3 x^2 + b_4 x^3) + m_i \delta_p (c_1 + c_2 x)]^{1/3}} \tag{49}$$

where

$$a_1 = 2 \quad a_2 = -\frac{28}{15} \quad a_3 = -\frac{1}{3} \tag{50}$$

$$b_1 = \frac{4}{3} \quad b_2 = -2 \quad b_3 = \frac{8}{15} \quad b_4 = \frac{1}{3} \tag{51}$$

$$c_1 = \frac{1}{2} \quad c_2 = -\frac{8}{15} \tag{52}$$

$$\delta_N^* = \left(\frac{4k_f \Delta T z}{g h_{fg}' a^*}\right)^{1/4} \tag{53}$$

$$a^* = \frac{\rho_f(\rho_f - \rho_m^*)}{\mu_f} \tag{54}$$

$$l_i = \frac{2\tau_{if}}{(\rho_f - \rho_m^*)g} \tag{55}$$

$$m_i = \frac{360 f_m \rho_m (u_m - u_i)^2}{(\rho_f - \rho_m^*) g d} \tag{56}$$

$$x = \frac{\delta_p}{R}. \tag{57}$$

In equations (49) and (57), δ_p is an approximate condensate layer thickness, that is obtained neglecting interfacial shear stress.

$$\delta_p = \delta_N \frac{1.189}{(1 + a_1' x_N + a_2' x_N^2)^{1/4}}, \tag{58}$$

where δ_N is the traditional Nusselt film thickness given by

$$\delta_N = \left(\frac{4k_f \Delta T z}{g h_{fg} a}\right)^{1/4} \tag{59}$$

$$a = \frac{\rho_f(\rho_f - \rho_m)}{\mu_f} \tag{60}$$

$$a_1' = -\frac{4}{5} \quad a_2' = -\frac{1}{3} \tag{61}$$

$$x_N = \frac{\delta_N}{R}. \tag{62}$$

The results for δ obtained using expression (49) have been compared to the results obtained solving the transcendental equation (29), and both results proved to be very close. The differences were always less than 5%, and usual differences are around 1%.

3. RESULTS AND DISCUSSION

Recently, several experiments on measuring local condensation heat transfer coefficients inside vertical tubes with noncondensable gas present have been carried out. The papers of Peterson *et al.* [4], Ogg *et al.* [21], and more recently Siddique *et al.* [20] reported the measurement of the heat transfer coefficients for different conditions inside vertical tubes. The theory developed in this paper was compared first with the data of Vierow and Schrock [4, 9], for pressures below 1.5 bars and different concentrations of noncondensable gases. The comparison was performed in the turbulent regime, i.e. with Reynolds numbers of the steam–NC mixture above 2300.

In Table 1, the results are displayed for run numbers 4, 5, 7 and 8, with practically the same pressure in all of them, and different NC mass fractions. In this case the calculations were performed without taking into account the mist formation ($C_{mist} = 1$) and waviness ($C_w = 1$). It was observed that the theoretical data follows pretty well the behavior of the experimental ones. The heat transfer coefficients diminish with the mixture Reynolds numbers for $z = 3.175 \times 10^{-2}$ m of runs 7 and 8. In these two cases the NC mass fractions and pressures have almost the same values, so the differences in the interfacial shear stresses arise from the differences in the local mixture velocities.

Now, the degradation in the heat transfer coefficients produced by the noncondensable gases can be observed comparing the runs 4 and 8 at $z = 15.24 \times 10^{-2}$ m with almost equal pressures and mixture Reynolds numbers, but different NC mass fractions, equal to 0.021 and 0.0575, respectively. In this case the heat transfer coefficients are smaller for the case with higher NC mass fraction.

Some authors like Mori and Hijakata [27] and Peterson [4], use the mist coefficient to account for the augmentation in sensible heat transfer due to mist formation, because the mist formation significantly increases the effective specific heat of the gas–vapor mixture increasing the effective Prandtl number. Our calculations show that in the turbulent region this coefficient is not very important. To check this, we have performed several calculations with the same model parameters that were used in the previous calculation of Table 1, but now the mist coefficient was varied from 1 to 5. We found that the influence of this coefficient was completely negligible at Reynolds numbers of the mixture above 4000, and smaller than 1% in the range of mixture Reynolds numbers between 2300 and 4000 for all the runs. So in the turbulent region, local heat transfer calculations can be performed without taking credit of mist formation ($C_{mist} = 1$).

Another factor that needs to be discussed is the wavy coefficient C_w, which appears in equation (42). This factor is used by some authors like Peterson *et al.* [4] to account for the enhancement in Sherwood number due to film waviness. For this reason, in the next calculation we take credit of the waviness coefficient and make $C_w = 1.2$ as recommended by Peterson *et al.* [4]; again, we use the same model parameters of the previous calculations without taking into account the mist formation ($C_{mist} = 1$).

The effect was to increase the value of the heat

Table 1. Local heat transfer coefficients of the model for run 4, 5, 7, 8. See ref. [9]. h_t(exp) and h_t(th) are the experimental and theoretical heat transfer coefficients. The model values were obtained with $C_2 = 0.023$, $C_{mist} = 1$, and $C_w = 1$

Run	$p \times 10^5$	$z \times 10^{-2}$	w_a	Re_m	h_t(exp)	h_t(th)	f	Error %
4	1.058	3.175	0.0103	11646	13665	14131	0.965	−3.5
4	1.058	3.81	0.0107	11122	13353	13217	1.008	−0.8
4	1.058	5.08	0.0115	10416	12196	11660	1.044	4.23
4	1.058	10.16	0.0155	7692	8121	8000	1.01	1.3
4	1.058	15.24	0.0210	5629	5716	6051	0.943	−6.0
4	1.058	20.32	0.0288	4050	4105	4737	0.865	−15.6
4	1.058	24.13	0.0369	3119	3121	3733	0.834	−19.8
5	1.03	3.175	0.0274	7184	7594	9363	0.809	−23.5
5	1.03	3.81	0.0285	6903	7316	8770	0.833	−20
5	1.03	5.08	0.0307	6368	6709	7765	0.862	−15.9
5	1.03	10.16	0.0421	4578	4823	5161	0.932	−7.1
5	1.03	15.24	0.0584	3222	3409	3138	1.08	7.7
7	1.024	3.175	0.0303	7142	9413	10024	0.937	−6.6
7	1.024	3.81	0.0316	6844	9121	9370	0.972	−2.9
7	1.024	5.08	0.0342	6281	8314	8239	1.007	0.7
7	1.024	10.16	0.0479	4404	5705	5190	1.09	8.8
7	1.024	15.24	0.0683	2997	3932	2936	1.33	25
8	1.077	3.175	0.0290	11871	14409	13554	1.06	5.7
8	1.077	3.81	0.0300	11439	13637	12590	1.08	7.5
8	1.077	5.08	0.0322	10617	12271	11066	1.10	9.6
8	1.077	10.16	0.0430	7836	8075	7250	1.11	10
8	1.077	15.24	0.0575	5730	5695	4935	1.15	13
8	1.077	20.32	0.0775	4117	3579	2718	1.31	23
8	1.077	24.13	0.0975	3172	2778	1672	1.65	39

transfer coefficients in every run, and higher relative errors were obtained in all of them except for run 8, which improved its results, and for run 4 which was not very much affected. Since run 8 was the one with higher condensate and mixture Reynolds numbers, and since according to Brodkey [30], Miles [31], and Hewitt [32] at a sufficiently high gas velocity the initially stable film becomes wavy, this result suggested that wavy effects were important for run 8, and thus the waviness coefficient C_w should depend on both mixture Reynolds number and condensate Reynolds number. Therefore it should not be taken as a constant. In Table 2 we show the results obtained for run 8, with $C_w = 1.2$.

We have also compared our results with experimental ones by Siddique *et al.* [20, 26]. In order to perform this comparison, a tube simulator has been developed based on the previous model which computes all the relevant state variables at several axial positions, as condensation proceeds along the tube. The calculation procedure starts at the tube inlet, where given the inlet conditions of temperature, steam mass flow rate, noncondensable mass fraction and wall temperature, the other relevant state variables are calculated.

The tube is then divided into an arbitrarily great number of elements of length Δz, chosen by the user. The steam mass flow rate $m_v(j+1)$ entering into element $j+1$ is calculated by means of the expression

$$m_v(j+1) = m_v(\text{inlet}) - \sum_{i=1}^{j} 2\pi R \left(\frac{d\Gamma}{dz}\right)_i \Delta z, \quad (63)$$

where m_v(inlet) is the inlet steam mass flow rate to the tube. The condensation rate per unit area $(d\Gamma/dz)_i$ at the element i, is calculated at the middle of the element in order to achieve better results. As steam condensates along the tube, the noncondensables mass fraction is recalculated at each element on account of the new value of the steam mass flow rate for that element.

It is also interesting to mention that at each element j, the diffusion layer model developed in previous sections is applied, along with the proper boundary conditions for that element that in turn are obtained as the calculation proceeds along the tube.

Our results for the air–steam case resolved in run number 24 have been compared with experimental data by Siddique *et al.* [20, 26]. In this experiment the internal diameter was 46 mm, the inlet steam mass flow rate was 0.0057 kg s^{-1}, the noncondensable mass fraction at the tube inlet was w_a(air) = 0.11, and the inlet mixture temperature 120°C. In Fig. 5 the experimental heat transfer coefficients measured by Siddique *et al.* are displayed, together with our theoretical results, represented by a continuous line.

As it can be seen, near the tube inlet the heat transfer coefficients change sharply with distance. This sudden change is due mainly to the fact that interfacial shear stress effects on the condensate film thickness are very important near the tube inlet, because the mixture Reynolds number is very high. Moreover, these high values of the interfacial shear stress acting on the liquid are increased by the suction of mass effect, also included in the model, thus producing reductions in

Table 2. Local heat transfer coefficients of the model for run 4, 5, 7, 8. See ref. [9]. h_t(exp) and h_t(th) are the experimenta and theoretical heat transfer coefficients. The model values were obtained with $C_2 = 0.023$, $C_{mist} = 1$ and $C_w = 1.2$

Run	$p \times 10^5$	$z \times 10^{-2}$	w_a	Re_m	h_t(exp)	h_t(th)	f	Error %
4	1.058	3.175	0.013	11646	13665	14253	0.956	−4.4
4	1.058	3.82	0.0107	11122	13353	13330	1.0	−0.03
4	1.058	5.08	0.0115	10416	12196	11760	1.035	3.41
4	1.058	10.16	0.0155	7692	8121	8092	1.002	0.2
4	1.058	15.24	0.0210	5629	5716.5	6159	0.926	−7.9
4	1.058	20.32	0.0288	4050	4105.9	4903	0.83	−19.6
4	1.058	24.13	0.0369	3119	3121	4034	0.77	−29.47
5	1.03	3.175	0.0274	7184	7594	9882.6	0.76	−30
5	1.03	3.81	0.0285	6903	7316	9223	0.79	−26
5	1.03	5.08	0.0307	6368	6709	8166	0.82	−21
5	1.03	10.16	0.0421	4578	4823	5575	0.86	−15.7
5	1.03	15.24	0.0584	3222	3409	3678	0.925	8
7	1.024	3.175	0.0303	7142	9413.7	10555	0.87	−12
7	1.024	3.81	0.0316	6844	9121.1	9896	0.92	−8.6
7	1.024	5.08	0.0342	6281	8314.8	8705	0.95	−4.8
7	1.024	10.16	0.0479	4404.3	5705	5677	1.00	0.3
7	1.024	15.24	0.0683	2997	3932	3455	1.1	11.98
8	1.077	3.175	0.0290	11871	14409	14046	1.02	2.3
8	1.077	3.81	0.0300	11439	13637	13045	1.04	4.1
8	1.077	5.08	0.0322	10617	12271	11466	1.07	6.3
8	1.077	10.16	0.0430	7836	8075.3	7615.6	1.06	5.5
8	1.077	15.24	0.0575	5730	5695.3	5402.5	1.052	4.9
8	1.077	20.32	0.0775	4117	3579.8	3234.6	1.10	9.4
8	1.077	24.13	0.0975	3172	2778.8	2032	1.36	26

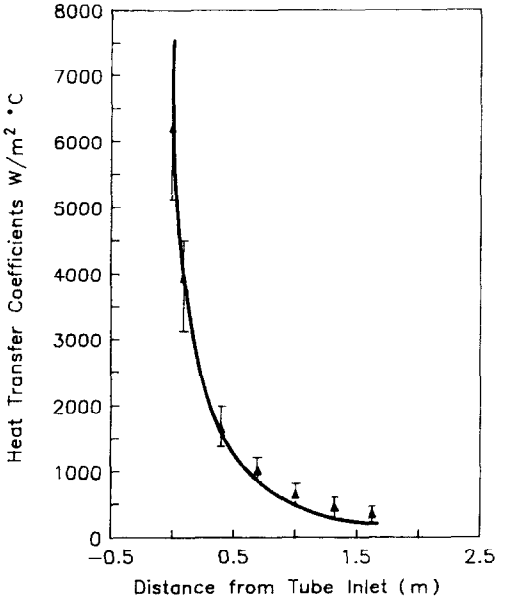

Fig. 5. Variation of heat transfer coefficients along the length of the condenser, with steam inlet flow rate 0.0057 kg s^{-1}, $T_{inlet} = 120$°C, and noncondensables mass fraction $w_a = 0.11$. ▲ Experimental points from Siddique *et al.* [26]. The continuous line shows the theoretical prediction.

the condensate layer thickness which tend to increase the local heat transfer coefficient. One observes in Fig. 5 that the theoretical results follow pretty well the experimental data in the turbulent region.

4. CONCLUSIONS

In this paper, a model has been developed for annular filmwise condensation inside vertical tubes when noncondensable gases are present. It was seen that in the turbulent region and at high Reynolds number the heat transfer coefficients strongly depend on the interfacial shear stresses which in turn depend on the correlation used to calculate the interfacial friction factors; the most popular is the Wallis' relation [23], which is the one used in this paper. However, as mentioned by Hewitt in ref. [24], better relations are needed for the determination of the interfacial friction factor at high pressures [25, 29].

The model developed in this paper provides good results in the turbulent region and with moderate mass fractions of noncondensable gases, ranging from 1 to 10%. In order to reduce the time spent in the iteration process, and to simplify the calculations, an approximate procedure has been developed. The latter provides the condensate film thickness without need of iterations to solve the transcendental equation (29). In this way equation (49), obtained in Section 2, development of the models, gives errors of less than 2% in the turbulent region, as it has been checked by solving this equation exactly by the secant iteration algorithm [28]. This fact is important for large simulation computational codes [33], where one of the parts is a condenser which needs to be simulated properly in a no-time-consuming way.

The model developed accounts for: (i) shear stresses produced by concurrent downflow, (ii) condensation

effects on sensible heat transfer and interfacial shear stresses, (iii) noncondensable gas effect on the heat transfer coefficients. Moreover, the influence of the condensation process on the Sherwood number has been taken into account. This influence was studied by Ackermann, and was applied by Wang and Tu [1] to downflow condensation in vertical tubes. In our case the same correction is applied, because the values of parameter ϕ_a, which appears in equation (42), were larger than 2 in the turbulent region. This result was verified by fitting the relation Sh/Sh_0 to the numerical results by Yeroshenko *et al.*, displayed in ref. [1] for values of ϕ_a less than 2, but using the Ackermann expression for ϕ_a larger than 2. The results obtained practically coincided with those calculated using the Ackermann expression in all ranges, which confirms that the parameter ϕ_a is greater than 2 in the turbulent region.

In summary, the theoretical predictions have been compared with the experimental results by Vierow and Schrock [9], see Table 1, and the agreement in the turbulent region is very good. They have also been compared to the experimental results by Siddique *et al.* [20, 26], and the agreement is excellent in all the cases. In Fig. 5 the theoretical and experimental heat transfer coefficients (HTC) are displayed vs the axial distance from the tube inlet. Note that the model predicts pretty well the sharp variation in the HTC with distance through the first 0.5 m. In this case, the noncondensables mass fraction is 0.11 at the entrance, therefore this means that higher NC mass fractions are attained as condensation proceeds along the tube, and the noncondensables model provides good results in all these cases.

Mist formation and wavy effects are included in the model by empirical coefficients, though a work is under way to include these effects in a more rigorous way. Some preliminary results are discussed in the previous section.

Acknowledgements—The authors are indebted to Jim Fitch, K. Vierow and B. Shiralkar for suggesting the study subject, and to UNESA for its support to develop this work.

REFERENCES

1. Chao-Yang Wang and Chuang-Jing Tu, Effects of non-condensable gas on laminar film condensation in a vertical tube. *Int. J. Heat Mass Transfer* **31,** 2339–2345 (1988).
2. A. P. Colburn and O. A. Hougen, Design of cooler condensers for mixtures of vapours with non-condensing gases. *Ind. Engng Chem.* **26,** 1178–1182 (1934).
3. J. G. Collier, *Convective Boiling and Condensation* (2nd Edn), pp. 323–340. McGraw-Hill, New York (1981).
4. P. F. Peterson, V. E. Schrock and T. Kageyama, *Diffusion Layer Theory for Turbulent Vapor Condensation with Non Condensable Gases*, HTD Vol. 197, *Two-Phase Flow and Heat Transfer*, ASME (1992).
5. W. Nusselt, Die oberflachen kondensation des waserdampfles, *Z. Ver. Dt. Ing.* **60,** 541–546 (1916).
6. W. J. Minkowycz and E. M. Sparrow, Condensation heat transfer in the presence of noncondensables, interfacial resistance, superheating, variable properties, and diffusion, *Int. J. Heat Mass Transfer* **9,** 1125–1144 (1966).
7. E. M. Sparrow, W. J. Minkowycz and M. Saddy, Forced convection condensation in the presence of non-condensables and interfacial resistance, *Int. J. Heat Mass Transfer* **10,** 1829–1845 (1967).
8. T. Kageyama, P. F. Peterson and V. E. Schrock, Diffusion layer modeling for condensation in vertical tubes with noncondensable gases, *Nucl. Engng Des.* **141,** 289–302 (1993).
9. K. M. Vierow and V. E. Schrock, Condensation in a natural circulation loop with noncondensable gases, part 1—heat transfer, in *Proc. Int. Conf. Multiphase Flows*, Tsukaba, Japan, September (1991).
10. K. M. Vierow, Behavior of steam–air systems condensing in concurrent vertical downflow, MSc. thesis, University of California, Berkeley (1990).
11. P. J. Vernier and P. Solignac, A test of some condensation models in the presence of noncondensable gases against the ecotra experiment, *Nucl. Technol.* **77,** 82–91 (1987).
12. G. F. Hewitt, Annular two-phase flow. In *Two Phase Flow and Heat Transfer with Application to Nuclear Reactor Problems*, pp. 49–66. Hemisphere, Washington, DC (1978).
13. G. F. Hewitt, *Introduction to Two-Phase Heat Transfer*, pp. 69–87. Hemisphere, Washington, DC (1978).
14. G. F. Hewitt, *Heat Transfer in High Quality Two Phase Flows*, pp. 111–132. Hemisphere, Washington, DC (1978).
15. V. M. Borishanski, D. I. Volkov, N. I. Ivashchenko, O. P. Krektunov, N. M. Fishman, and I. N. Chirkiv, Shell-side coefficient of heat transfer from steam contaminated with non-condensable gases, *Heat Transfer-Soviet Res.* **14,** 15 (1982).
16. V. M. Borishanski, D. I. Volkov, N. I. Ivashchenko, L. A. Vorontsova, Yu. T. Illarionov, O. P. Kretunov, A. P. Borkov, G. A. Makarova and I. A. Alokseyev, Heat transfer from steam condensing inside vertical pipes and coils, *Heat Transfer-Soviet Res.* **10,** 44–57 (1978).
17. V. M. Borishanski, D. I. Volkov, N. I. Ivashchenko, O. P. Kretunov, L. A. Vorontsova, G. A. Makarova and N. M. Fishman, Effect of uncondensable gas content on heat transfer in steam condensation in a vertical tube, *Heat Transfer-Soviet Res.* **9,** 35–42 (1977).
18. B. L. Kreiden, I. L. Kreiden and V. A. Lokshin, Experimental investigation of hydraulic resistance with condensation of steam down-flow inside a vertical tube, *Thermal Engng* **31,** 21–24 (1984).
19. A. A. Dehbi, Analytical and experimental investigation of the effects of non-condensable gases on steam condensation under turbulent natural convection conditions, Ph.D. dissertation, M.I.T., Department Nuclear Engineering (1990).
20. M. Siddique, M. W. Golay and M. S. Kazimi, Local heat transfer coefficients for forced convection of steam in a vertical tube in the presence of a noncondensable gas, *Nucl. Technol.* **102,** 386–402 (1993).
21. D. G. Ogg, Vertical downflow condensation heat transfer in gas-steam mixtures, M.S. thesis, Department of Nuclear Engineering, University of California, Berkeley (1991).
22. R. S. Silver, An approach to a general theory of surface condensers, *Proc. Inst. Mech. Engrs* **178**(14), 339–376 (1964).
23. G. B. Wallis, *One-Dimensional Two Phase Flow*, McGraw-Hill, New York (1969).
24. D. P Spalding, *Convective Mass Transfer*. McGraw-Hill, New York (1963).
25. G. Hetsroni, *Handbook of Multiphase Systems*, pp. 2–64, 2–71. Hemisphere, Washington, DC (1982).
26. M. Siddique, M. W. Golay and M. S. Kazimi, Theoretical modeling of forced convection condensation of

steam in a vertical tube in the presence of a non-condensable gas, *Nucl. Technol.* **166,** 202–214 (1994).
27. Y. Mori and K. Hijakata, Free convective condensation heat transfer with noncondensable gas on a vertical surface, *Int. J. Heat Mass Transfer* **16,** 2229–2240 (1973).
28. W. H. Press, S. A. Teukolski, W. T. Vetterling and B. P. Flannery, *Numerical Recipes in FORTRAN*. Cambridge University Press, Cambridge (1992).
29. P. B. Whalley and G. F. Hewitt, The correlation of liquid entrainment fraction and entrainment rate in annular two phase flow, Report AERE_R9187, UKAEA (1978).
30. R. S. Brodkey, *The Phenomena of Fluid Motion*, pp. 456–465, 539–618. Addison-Wesley, Reading, MA (1967).
31. J. W. Miles, On the generation of surface waves by shear flows, *J. Fluid Mech.* **13,** 433–448 (1962).
32. G. F. Hewitt, Disturbance waves in annular two phase flow, *Proc. Inst. Mech. Engrs* **184,** 142–150 (1969).
33. TRAC-BF1/MOD1 : An Advanced Best-Estimate Computer Program for BWR Accident Analysis, Model Description, NUREG/CR-4356, U.S. NRC (1992).
34. G. Ackermann, Simultaneous heat and mass transfer with large temperature and partial pressure differences, *Ver. deutscher Ing. Forch.* **8,** 1–16 (1937) (in German).
35. W. M. Rohsenow, Heat transfer and temperature distribution in laminar film condensation, *Trans. ASME* **78,** 1645–1648 (1956).